Journal of Taibah University Medical Sciences (2024) 19(6), 1119–1129

Taibah University

Journal of Taibah University Medical Sciences

www.sciencedirect.com

Original Article

Comparative analysis of hydrazinyl coumarin derivative incorporation in resin-modified and conventional glass ionomer cement

Nor A.F. Azlisham, MSc [a], Fatimah S.A. Rahman, PhD [a], Zuliani Mahmood, DClinDent [b,*], Dasmawati Mohamad, PhD [a], Yanti Johari, DClinDent [c] and Ola B. Al-Batayneh, MDSc [d]

[a] *Unit of Biomaterials, School of Dental Sciences, Universiti Sains Malaysia Health Campus, Kubang Kerian, Kelantan, Malaysia*
[b] *Unit of Paediatric Dentistry, School of Dental Sciences, Universiti Sains Malaysia Health Campus, Kubang Kerian, Kelantan, Malaysia*
[c] *Unit of Prosthodontics, School of Dental Sciences, Universiti Sains Malaysia Health Campus, Kubang Kerian, Kelantan, Malaysia*
[d] *Department of Preventive Dentistry, Faculty of Dentistry, Jordan University of Science and Technology, Irbid, Jordan*

Received 19 July 2024; revised 9 October 2024; accepted 11 November 2024; Available online 20 November 2024

الملخص

أهداف البحث: هدفت الدراسة إلى إجراء تحليل مقارن لتأثيرات دمج مشتق الكومارين الهيدرازيني في إسمنت أيونومر الزجاج المعدل بالراتنج والتقليدي على معدلات تحررهما وخصائصهما المضادة للبكتيريا.

طرق البحث: استخدم إسمنت أيونومر الزجاج المعدل بالراتنج فوجي الثاني وإسمنت أيونومر الزجاج التقليدي عالي الفلوراید فوجي السابع كمجموعات ضابطة. تم تصنيع مشتق الكومارين الهيدرازيني داخليا، ودمجه في كلا النوعين بنسب وزنية واحد وإثنين بالمئة، وتحليله كيميائيا باستخدام مطيافية الأشعة تحت الحمراء. ثم تم تقييم معدلات تحرر مشتق الكومارين الهيدرازيني والفلوراید باستخدام مطياف الأشعة فوق البنفسجية المرئية ومقياس الفلوراید على التوالي. تم تقييم الخصائص المضادة للبكتيريا ضد المكورات العقدية الدموية باستخدام طريقة الانتشار في الأجار وقياس عكارة النمو البكتيري، متبوعا بملاحظة الشكل البكتيري باستخدام المجهر الإلكتروني الماسح. تم تحليل البيانات إحصائيا باستخدام تحليل التباين أحادي الاتجاه واختبار بونفيروني البعدي.

النتائج: أكدت أطياف الأشعة تحت الحمراء وجود مشتق الكومارين الهيدرازيني في مصفوفات الإسمنت. تم تحرر المشتق بنجاح من كلا النوعين بكلتا النسبتين الوزنيتين. لوحظ تحرر أعلى للفلوراید ومناطق تثبيط أكبر مقارنة بالمجموعات الضابطة، مع تأثير أكثر أهمية في النوع المعدل بالراتنج. بالإضافة إلى ذلك، أدى دمج المشتق إلى إبطاء نمو المكورات العقدية الدموية وأظهر تغيرات ملحوظة في شكل البكتيريا خاصة في النوع المعدل بالراتنج.

الاستنتاجات: أدى دمج مشتق الكومارين الهيدرازيني في كلا نوعي الإسمنت إلى تحسين تحرر الفلوراید وتعزيز الأنشطة المضادة للبكتيريا، مع ملاحظة تأثير أكثر أهمية في النوع المعدل بالراتنج مقارنة بالنوع التقليدي.

الكلمات المفتاحية: الخصائص المضادة للبكتيريا؛ مشتق الكومارين؛ تحرر الفلوراید؛ إسمنت أيونومر الزجاج؛ إسمنت أيونومر الزجاج المعدل بالراتنج؛ المكورات العقدية الدموية

Abstract

Objective: The study aimed to conduct a comparative analysis of the effects of incorporating hydrazinyl coumarin derivative (HCD) in resin-modified (RMGIC) and conventional glass ionomer cement (cGIC) on their release profiles and antibacterial properties.

Method: Resin-modified GIC, Fuji II LC (F2) and high-fluoride cGIC, Fuji VII (F7) were used as controls. HCD was synthesized in-house, incorporated into both RMGIC and cGICs at 1 % and 2 % weight percentages (w/w), and chemically analyzed using Fourier transform infrared (FTIR) spectroscopy. Then, the F2 containing HCD (GIC-HCD F2) and F7 containing HCD (GIC-HCD F7) were evaluated for HCD and fluoride release profiles using UV Visible spectrophotometer and pH/ISE benchtop fluoridemeter, respectively. The antibacterial properties were assessed against *Streptococcus sanguinis*

* Corresponding address: Unit of Paediatric Dentistry, School of Dental Sciences, Universiti Sains Malaysia Health Campus, 16150 Kubang Kerian, Kelantan, Malaysia.
E-mail: zuliani@usm.my (Z. Mahmood)

Peer review under responsibility of Taibah University.

Production and hosting by Elsevier

 https://doi.org/10.1016/j.jtumed.2024.11.003

using the agar well diffusion method and measurement of bacterial growth turbidity, followed by the observation of the bacterial morphology using scanning electron microscope. The data were statistically analyzed using one-way ANOVA and Bonferroni post-hoc tests.

Results: The FTIR spectra confirmed the presence of HCD in the GIC-HCD matrices. HCD was successfully released from both GIC-HCD F2 and GIC-HCD F7 matrices at both weight percentages. Higher fluoride release and inhibitory zones were observed compared to the control groups, with GIC-HCD F2 having a more significant effect than GIC-HCD F7. Additionally, the incorporation of HCD slowed down the growth of *Streptococcus sanguinis* and showed remarkable changes in bacterial shape specifically on GIC-HCD F2.

Conclusion: The incorporation of HCD into both RMGIC and cGIC improved fluoride release and enhanced the antibacterial activities, with a more significant effect observed in RMGIC compared to cGIC.

Keywords: Antibacterial properties; Coumarin derivative; Fluoride release; Glass ionomer cement; Resin-modified glass ionomer cement; *Streptococcus sanguinis*

Introduction

Modern dental restorative materials restore the function and integrity of missing tooth structures and offer preventive and therapeutic effects against oral diseases, such as dental caries. For instance, fluoride-releasing restorative materials protect tooth structures and adjacent teeth against demineralization, enhance remineralization of initial caries lesions and increase resistance to subsequent acid attacks by decreasing the metabolic activities of pathogenic oral biofilms.[1,2] Glass ionomer cement (GIC) is reportedly the most efficient in combating secondary caries amongst fluoride-releasing restorative materials that are essential for preventing restoration failures.[1,3]

GIC possesses several desirable characteristics, such as biocompatibility with pulp and gingival tissue, adherence to tooth structures, thermal compatibility with tooth enamel and anti-cariogenic capabilities.[4] Resin-modified GIC (RMGIC) was introduced to overcome the disadvantages of conventional GIC (cGIC), which include low mechanical properties, high moisture sensitivity, inferior translucency and handling facilities. The cGIC and RMGIC contain the same essential components, fluoroaluminosilicate glass powder and polyacrylic acid, while RMGIC comprises an additional resin, hydroxyethyl methacrylate (HEMA).[5]

Antimicrobial agents-incorporated GIC implementations as therapeutic agents in minimizing the risk of caries and pulp damage have been extensively studied.[6–9] Nevertheless, most antimicrobial agents reduce the mechanical properties of GIC. Moreover, although higher concentrations demonstrated more effects, the antimicrobial agents might also inhibit fluoride release.[10] Adding antimicrobial agents to dental restorative materials could potentially target specific cariogenic species.[11] Nonetheless, the search for antimicrobial agents with synergistic or complementary modes of action to fluoride-releasing GIC without compromising their physical and mechanical properties is still imperative.[12]

The coumarins are extremely structurally variable owing to the different types of substitutions in their basic structures, which might influence their biological activities.[13] Coumarins contain 1,2-benzopyrone, which is an essential group of organic compounds derived from extracted plants, animals and microorganisms, or synthetic sources.[14,15] Natural and synthetic coumarins have been demonstrated to be useful in several fields, including their potential as antibacterial agents against both gram-positive and -negative bacteria,[15,16] antioxidant,[17] antifungal[18] and anti-inflammatory[19] properties. The promising features of coumarin derivatives emerge as a suitable option for further investigation to be incorporated with GIC. In this study, the coumarin derivative used, hydrazinyl coumarin derivative (HCD) (Figure 1), is a synthetically derived organic compound from a 3-acetylcoumarin and thiosemicarbazide derivative mixture.[20] The 3-acetylcoumarin has demonstrated antimicrobial properties,[21–23] while thiosemicarbazide derivatives recorded good inhibitory properties against microorganisms affecting dental caries, including *Streptococcus mutans* and *Streptococcus sanguinis*.[24]

To date, the information on the incorporation of HCD in both RMGIC and cGIC remains limited. While the incorporation of HCD as an antibacterial agent at different weight percentages may offer therapeutic effects, it may also potentially compromise fluoride release and antibacterial properties. Therefore, the study aims to conduct a comparative analysis of the effects of incorporating HCD at 1 % and 2 % weight percentage (w/w) in RMGIC and cGIC on the release profiles of HCD and fluoride, as well as the antibacterial properties. Understanding these properties is crucial for anticipating long-term performance and broadening their potential applications, particularly in dental restoration.

Materials and Methods

Sample preparation

The present study used resin-modified Fuji II LC (GIC F2) and high fluoride conventional Fuji VII (GIC F7) (GC Corporation, Tokyo, Japan) GIC dental restorative materials as control groups. The compositions and particle sizes of the materials are listed in Table 1.

HCD was synthesized in-house through a Schiff base reaction, following the method described by Rahman et al..[20] Briefly, a mixture of 3-acetylcoumarin and thiosemicarbazide derivative was heated under reflux at 80–120 °C with 25–30 drops of glacial acetic acid added as the catalyst to obtain the HCD. Subsequently, 1 % and 2 % (w/w)

of the HCD were incorporated into the F2 and F7 GIC powder components to yield the GIC-HCD 1 and GIC-HCD 2 samples, respectively. Finally, liquid drops were added to the GIC-HCD before they were homogeneously mixed at powder-to-liquid ratio of 1:2 for F2 and 1:1 for F7, following the manufacturer's instructions.

Chemical analysis

The synthesized HCD, GICs and GIC-HCD at both weight percentages were first analyzed for their functional groups using Fourier transform infrared (FTIR) spectra. The spectra were recorded within the 4000−400 cm^{-1} range in the transmittance mode with KBr pellets and an FTIR Spectrometer (Shimadzu/IRTracer-100, Japan).

Release profiles

The HCD release

The HCD released by the GIC-HCD samples by soaking disc-shaped samples (5 mm diameter, 2 mm thick; n = 3/group) in 1 ml of 50 % articifial saliva (Pharmacy Department, Hospital Universiti Sains Malaysia) at 37 °C. The saliva was replaced with fresh artificial saliva at each incubation period. The amount of HCD released was measured hourly for the first 8 h and then daily for 30 days (720 h) using a microplate reader (SpectraMax MS, Molecular Device, USA) at a wavelength of 350 nm.

Fluoride release

Disc-shaped samples (5 mm diameter, 2 mm thick; n = 3/group) were prepared before they were individually immersed in 5 ml deionized water and stored in a water bath at 37 °C. The sample solutions were collected and replaced with fresh deionized water daily from day 1 to day 21. The fluoride ions released were measured by adding 5 ml of total ionic adjustment buffer II (TISAB II). The amount of fluoride released in the medium was determined using a pH/ISE benchtop meter with a fluoride ion selective electrode (ISE) [Thermo Orion, Massachusetts (USA)]. During this study, calibrations were performed daily using three fluoride standard solutions at 0.1, 1.0 and 10 ppm.

Antibacterial activities assessments

Bacterial strain

A loopful of *Streptococcus sanguinis* (*S. sanguinis*) (ATCC 10556) was reactivated in a brain-heart infusion (BHI) broth [Oxoid, United Kingdom (UK)]. The bacterial strain was grown anaerobically in a bacteriological incubator at 37 °C for 24 h. The bacterial suspension obtained was then adjusted to a density of approximately 0.5 McFarland standard and diluted to 1×10^6 CFU/ml with a densitometer [Grant-bio Den-1, United States of America (USA)].

Agar well diffusion

A 100 µl bacterial suspension was prepared and inoculated onto agar plates. Five mm diameter wells were made in each plate with sterile pipette tips. The prepared GIC-HCD samples (n = 3/group) were then aseptically loaded into the wells in a paste form to avoid contamination. The agar plates were incubated in a bacteriological incubator at 37 °C for 24 h. Following incubation, the inhibition zones of each sample were measured and recorded at three points.

Bacterial growth turbidity measurement

Three GIC-HCD samples per group (5 mm diameter, 2 mm thick) were prepared and immersed in a 5 ml BHI broth at 37 °C in a water bath (Julabo SW23, Germany) for 24 h. Following incubation, 2.5 ml of the eluents from each sample were filtered and mixed with 2.5 ml of the prepared bacterial suspension. The bacterial growth of *S. sanguinis* was measured by evaluating the hourly changes in optical density (OD) for 11 h with a densitometer (Grant-bio Den-1, USA). A growth curve was plotted based on the data.

Surface morphology of S. sanguinis *on the GIC-HCD*

The prepared GIC-HCD samples (5 mm diameter, 2 mm thick) were incubated in the bacterial suspension (0.5 McFarland standard equivalent to 1×10^6 CFU/ml) for 24 h. After incubation, the samples were rinsed with phosphate buffer saline (PBS), fixed in 4 % paraformaldehyde immediately for 4 h, followed by another rinse with PBS. The samples were then dehydrated with a series of low to high concentrations of ethanol solutions (50, 70, 90 and twice at 100 %) for 5 min in each solution, with 5 min intervals between treatments. After dehydration, the samples were left overnight in a desiccator at room temperature. The dehydrated samples were sputter-coated with gold and examined under a scanning electron microscope (Quanta 450 FEG, Fei, Netherland) at 10 000 × magnification with a 5 kV accelerating voltage.

Statistical analysis

The statistical analyses were performed using IBM SPSS Software version 23.0 (IBM Corporation, USA). Independent t-tests were performed to analyze the HCD release. The fluoride release and agar well diffusion data were analyzed with one-way analysis of variance (ANOVA) and post-hoc Bonferroni to determine the significant differences ($p < 0.05$) between the control GICs and GIC-HCD samples. The data were expressed as means and standard deviations.

Results

The FTIR spectra revealed the functional groups present in the synthesized HCD, GIC and GIC-HCD. The obtained

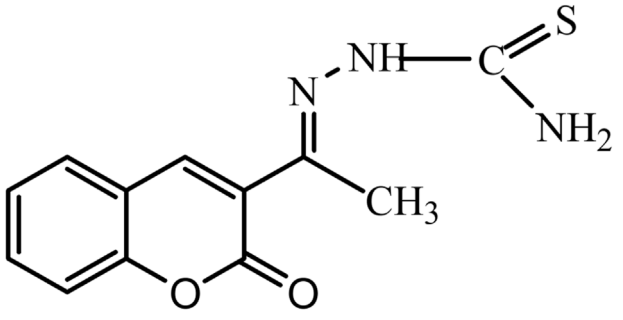

Figure 1: The chemical structure of HCD.

Table 1: The compositions of the dental restorative materials used in this study.

Material	Composition		Particle size
	Powder	Liquid	
Resin-modified GIC Fuji II LC	Fluoroaluminosilicate glass	Aqueous polycarboxylic acid, camphorquinone, hydroxyethylmetacrylate (HEMA)	~3.73 μm
High fluoride cGIC Fuji VII	Fluoroaluminosilicate glass	Polyacrylic and polybasic carboxylic acids	~6.31 μm

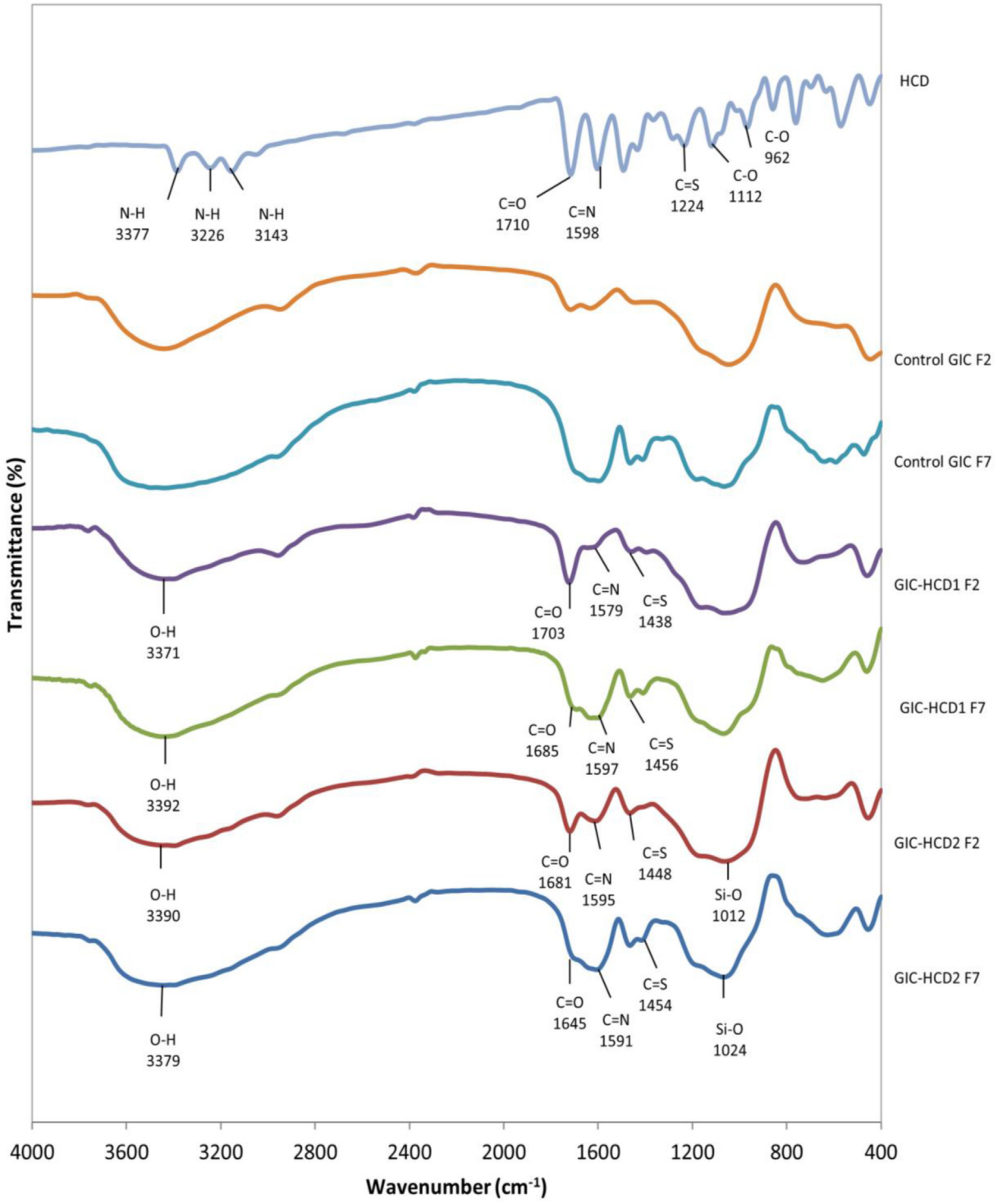

Figure 2: The FTIR spectra of the HCD, GICs and GIC-HCD.

spectra are illustrated in Figure 2. In HCD, the peaks at 3377, 3226 and 3143 cm^{-1} belonged to the NH and NH_2 amine groups. The peaks observed at 1710, 1598 and 1224 cm^{-1} denoted the presence of C═O, C═N and C═S, while peaks at 1112 and 962 cm^{-1} corresponded to the C−O group.

Upon incorporating HCD into GICs, similar spectra were observed between the GIC-HCD and the control groups. Broad peaks at 3371, 3390, 3392 and 3379 cm^{-1} recorded by GIC-HCD1 F2, GIC-HCD2 F2, GIC-HCD1 F7 and GIC-HCD2 F7 respectively, indicated the hydrogen bonded to O−H stretching vibration. These broad peaks presumably hindered the presence of amine groups in HCD, as the amount of HCD was only 1 % and 2 % (w/w) in the composition.

For F2, the peaks observed in GIC-HCD1 and GIC-HCD2 at 1703 and 1681 cm^{-1}, 1579 and 1595 cm^{-1}, and 1438and 1448 cm^{-1} denote the C═O, C═N and C═S groups, respectively. The peaks corresponding to C═O (1703 and 1681 cm^{-1}) and C═N (1579 and 1595 cm^{-1}) observed in the GIC-HCD1 F2 and GIC-HCD2 F2 were at higher intensities than their control groups, indicating chemical interactions between the GIC F2 and the HCD. For F7, despite their low intensities, the peaks recorded at 1685, 1597 and 1456 cm^{-1} (GIC-HCD1 F7) and 1645, 1591 and 1454 cm^{-1} (GIC-HCD2 F7) indicated the presence of C═O, C═N and C═S respectively. The peaks observed at 1012 cm^{-1} and 1024 cm^{-1} in both F2 and F7 were identified with the Si−OH stretching vibration, as described by Fareed and Stamboulis.[25]

The cumulative HCD release profile of GIC-HCD is illustrated in Figure 3. The amounts of HCD released from the GIC-HCD F2 and GIC-HCD F7 were dependent on the weight percentages of HCD added. The independent t-

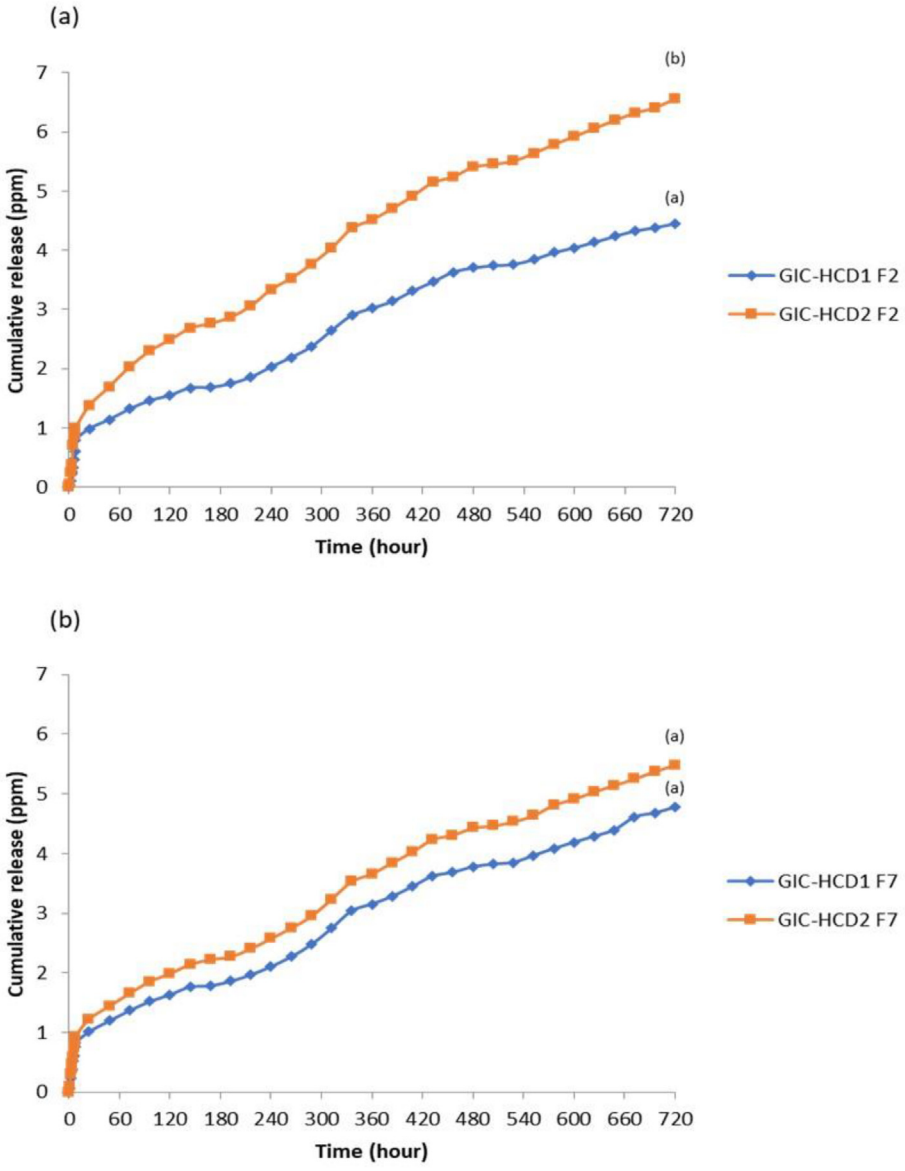

Figure 3: The cumulative HCD release profile of the GIC-HCD from (a) F2 (b) F7. Different superscript letters indicate significant differences within groups ($p<0.05$).

test performed detected a significant difference between the GIC-HCD1 F2 and GIC-HCD2 F2, while no significant difference was observed in GIC-HCD F7.

The incorporation of HCD into GIC-HCD F2 [Figure 4(a)] and GIC-HCD F7 [Figure 4(b)] increased the fluoride release. The release patterns observed by both materials were similar. The highest amount of fluoride was recorded on the first day, followed by a sharp decrease on day 2, with a slow and steady release observed from day 3 until day 21.

The GIC-HCD2 F2 showed a significant increase in fluoride release from day 1 to day 21 compared to its control group, however, the GIC-HCD1 F2 only demonstrated a significant difference on the first day. The GIC-HCD F7

Table 2: The inhibition zone of the control GICs, GIC-HCD1 and GIC-HCD2 against *S. sanguinis*.

Materials	Inhibition zone (mm)		
	Control GIC	GIC-HCD1	GIC-HCD2
F2	2.39 (0.65)[a]	4.85 (0.49)[b]	6.33 (0.05)[c]
F7	1.50 (0.63)[a]	2.10 (0.39)[a]	2.59 (0.22)[a]

The mean value and standard deviation are in parentheses. Different small letters in the same row are statistically different according to Bonferroni test ($p < 0.05$).

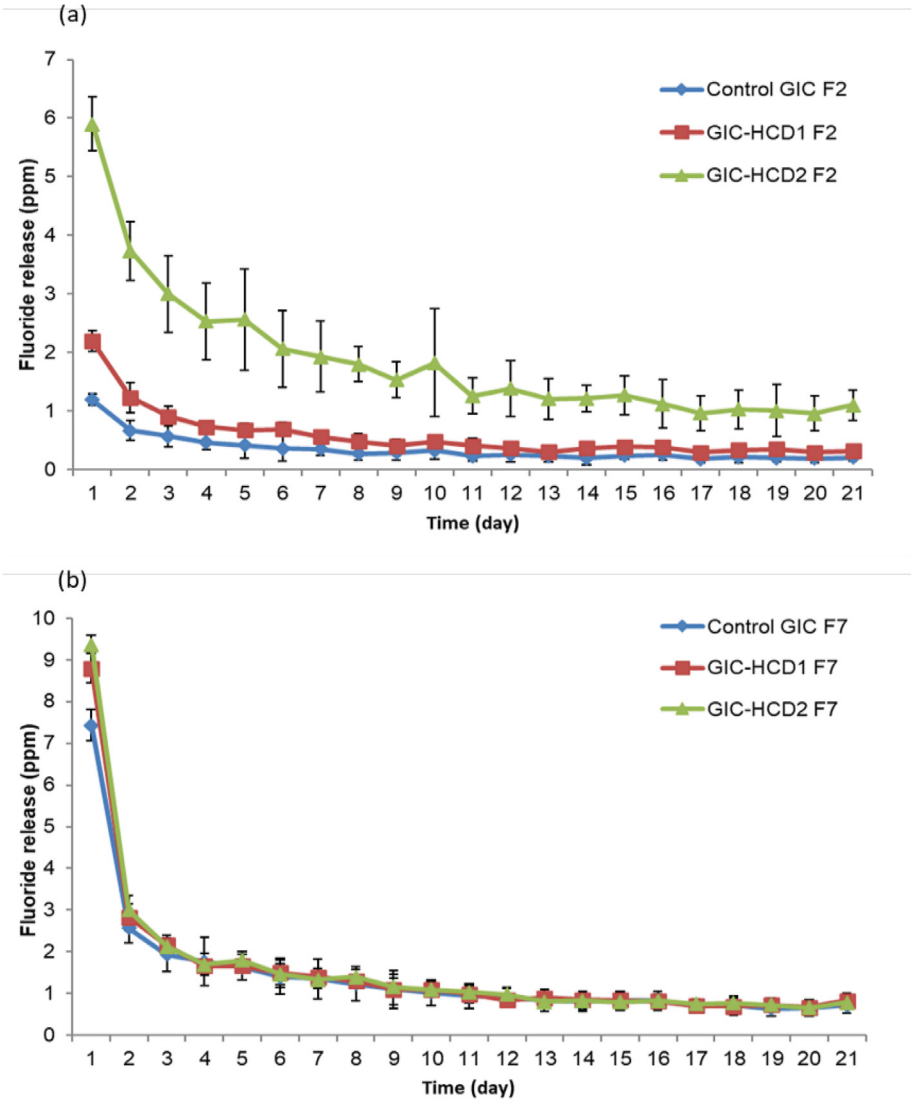

Figure 4: The fluoride release of the GIC-HCD and control GICs (a) F2 and (b) F7.

released significantly increased fluoride at both weight HCD percentages on day 1. Nevertheless, no significant fluoride release level was detected from day 2 onwards compared to its control GIC. The highest fluoride released by the GIC-HCD2 F2 and GIC-HCD2 F7 were 5.90 and 9.37 ppm, respectively.

The inhibition zone of the control GICs, GIC-HCD1 and GIC-HCD2 against *S. sanguinis* is shown in Table 2. In this study, antibacterial activities of the control GICs, GIC-HCD F2 and GIC-HCD F7 at 1 % and 2 % (w/w) against *S. sanguinis* were observed. The inhibition zone sizes produced by the GIC-HCD F2 increased significantly with the increase in HCD percentages compared to the control group. However, the inhibition zone increment observed in the GIC-HCD F7 samples was not significant compared to its control group.

The effects of incorporating HCD into the GICs on *S. sanguinis* growth were evaluated as a function of time. Figure 5(a) and 5(b) demonstrate the *S. sanguinis* growth turbidity measurement curves on the GIC-HCD F2 and GIC-HCD F7 and the control GICs during 11 h of incubation. All curves exhibited lag, log and stationary phases. A similar bacterial growth curve pattern was observed between the positive control, the GIC-HCD F2, GIC-HCD F7 and the control GICs.

The surface morphologies of *S. sanguinis* on the control GICs and GIC-HCD at 24 h of incubation are illustrated in Figure 6(a)–(f). Most *S. sanguinis* adhered to the control GIC of both samples when observed at 10 000 × magnification. Nevertheless, as the percentage of HCD increased, less *S. sanguinis* adhered to the GIC

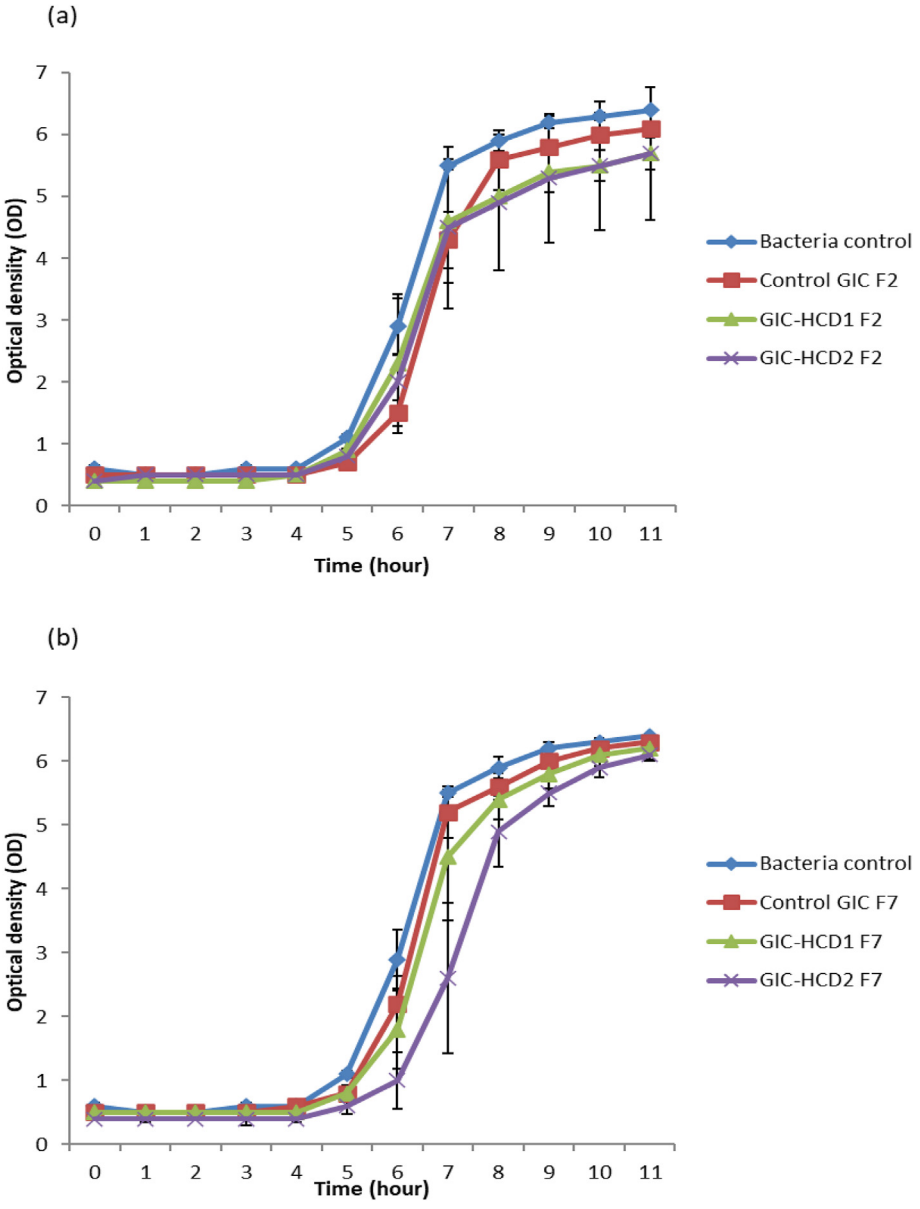

Figure 5: The growth turbidity measurement of *S. sanguinis* on the GIC-HCD and control GICs (a) F2 and (b) F7.

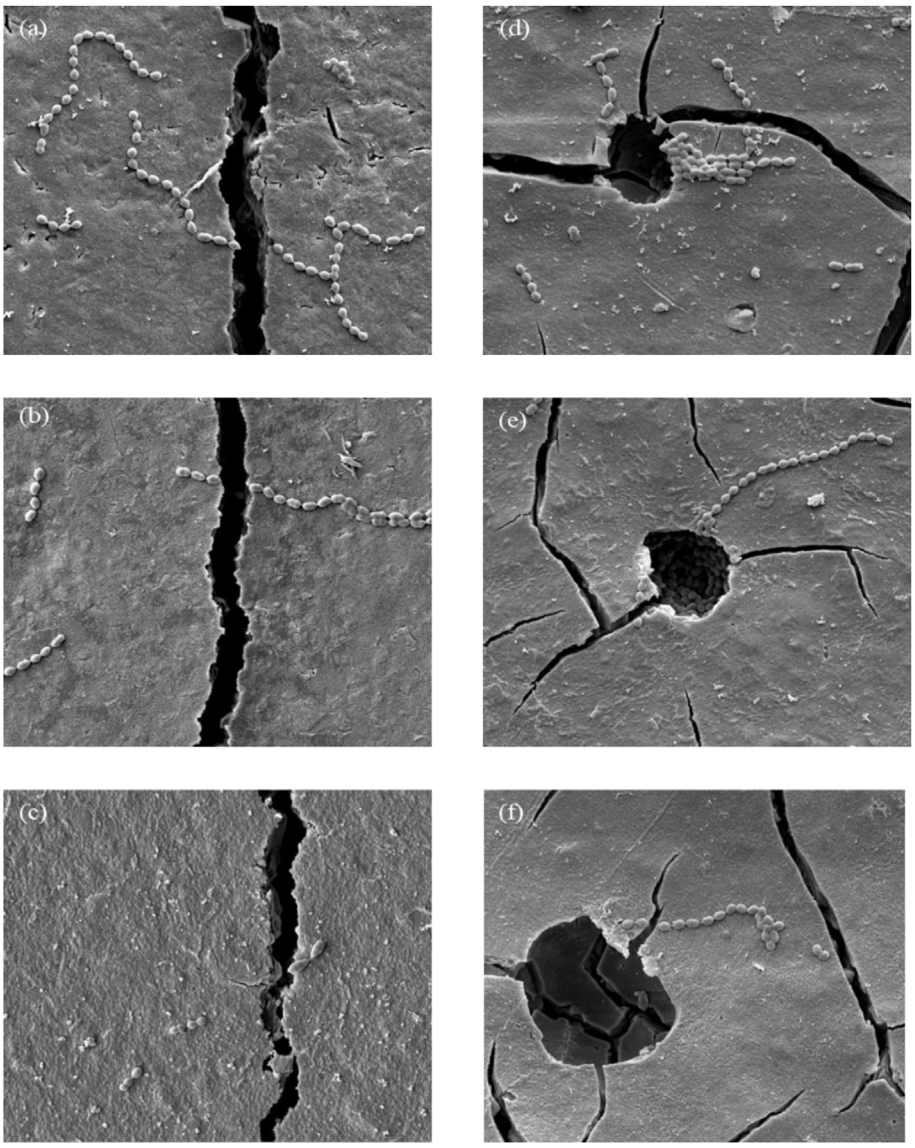

Figure 6: The SEM images of *S. sanguinis* adhesion on the (a) control GIC F2, (b) GIC-HCD1 F2, (c) GIC-HCD2 F2, (d) control GIC F7, (e) GIC-HCD1 F7 and (f) GIC-HCD2 F7 at 10 000 × magnification.

surfaces. The surface morphologies demonstrated that GIC-HCD exhibited greater antibacterial activity compared to GICs without HCD incorporation. The distribution of *S. sanguinis* on the samples also exhibited numerous single long-chain cocci, except GIC-HCD2 F2 [Figure 6(c)], which depicted the distribution of diplococci.

Discussions

The FTIR spectra confirm the successful incorporation of HCD into the GIC matrix, as evidenced by the intensified C═O and C═N groups. These interactions suggest that HCD forms chemical bonds with the GIC, likely influencing fluoride release by modifying the cross-linking density and enhancing the antibacterial properties of the GIC-HCD. Additionally, the broad peaks in the O−H region indicate that the hindered amine groups (N−H) may be involved in hydrogen bonding with the GIC matrix, which could potentially affect the overall stability of the GIC-HCD. Although these chemical interactions benefit fluoride release and antibacterial activity, they might also impact the setting reaction and mechanical properties of the GIC-HCD, highlighting the need for further optimization for clinical use.

HCD release refers to the migration of HCD solutes from their initial position within the GICs to the outer surface and into the release medium. The HCD release of both GICs in this study increased with increasing weight percentages (Figure 2). In the first 24 h, a rapid HCD release was recorded of approximately 1 ppm, attributable to the immediate dissolution of HCD. The rapid release was followed by a long period of linearity from the 48th h, presumably due to some remaining HCD, either chemically or physically bound to the GIC. The results of the present study were consistent with those reported by Palmer

et al.,[26] who observed a release pattern of chlorhexidine from GIC, recording an initial rapid elution of material that leveled off to a constant value.

Fluoride release is an essential feature of dental restorative materials because of its anti-cariogenic properties.[2] Since there is no fluorine element in HCD, the fluoride released from GIC-HCD matrices might have originated from the fluoroaluminosilicate glass. Fluoride is transported as metal cationic complexes as aluminum fluoride (AlF_2) and calcium fluoride (CaF_2) in the GIC matrices. Consequently, when more aluminum and calcium polyacrylate complexes are formed during the setting reaction, higher amounts of fluoride ions are released.[27] Meryon and Smith[28] reported that the release of fluoride from GIC was limited by the amount of sodium fluoride (NaF) and CaF_2 in the cement. In this study, the increased HCD percentage enhanced the amount of fluoride released. Thus, the incorporated HCD potentially allowed aluminum and calcium to form more complexes during the setting, contributing to the higher release of fluoride. Furthermore, the HCD possibly altered the setting reaction, which made the fluoride ions more mobile in the cement lattices.

The fluoride release pattern found in this study was consistent with the results reported by several other researchers.[29,30] Fluoride is released from GIC through three mechanisms; surface loss, diffusion through pores and cracks and bulk diffusion.[29] The highest amount of fluoride is released in the first 24 h, which is during the early setting of GIC.[31] This initial burst is presumably associated with the release of fluoride loosely bound to the cement, originating from the acid−base reactions between the glass components and polyalkenoic acid.[32] The initial burst reduces the viability of residual bacteria in the inner carious dentin and induces enamel/dentin remineralization,[33] which prevents secondary caries. The burst effect is probably due to an initial surface loss and constant fluoride released during the following days from the fluoride ions that diffuse through the cement pores and fractures. Bulk diffusions occur during the maturation period when the materials are in contact with the storage medium.[34]

Dental caries is a biofilm-mediated, diet-modulated, multifactorial, non-communicable and dynamic disease resulting in net mineral loss of dental hard tissues.[35] *Streptococccus sanguinis* was selected as the assessment bacteria in this study because this bacterium is among the first oral biofilm to colonize tooth surfaces[36,37] and develop primary and secondary caries. Long-lasting dental restoration relates to its ability to control microbial growth and surface colonization.[38]

Increased inhibition zones in GIC-HCD1 F2, GIC-HCD2 F2, GIC-HCD1 F7 and GIC-HCD2 F7 compared to their respective control groups (Table 2) were attributable to the HCD leaching from their GIC-HCD matrices. The smaller particles of GIC F2 (~3.73 μm) than GIC F7 (~6.31 μm) might explain the significant increase in the inhibition zones in GIC-HCD F2 compared to the control GIC, likely due to reduced cross-linking density within the GIC F2 matrix. Moreover, the HCD might also have reacted completely with the GIC F2, allowing the HCD to diffuse out more readily into the agar. The antibacterial activities could be accounted to the binding of the positively charged carbonyl (-C═O) and azomethine (-C═N-) groups from HCD on the negatively charged bacterial cell surface. Subsequently, the permeability of the cell membranes of the microorganisms was disrupted, leading to cell death. The azomethine groups also reportedly possess antibacterial effects.[24,39]

The inhibition zones observed in the control groups could be due to HCD and fluoride release. In this study, although the GIC F7 contains higher fluoride than the GIC F2, the inhibition zones in GIC F2 recorded a significant increase compared to GIC F7. The results could be explained by the release of hydrophilic monomer, HEMA, from the GIC F2, as HEMA has been reported to have antibacterial properties.[40]

The OD recorded by the GIC-HCD decreased with the increase in HCD percentages (Figure 4). The OD curves for the GIC-HCD were lower than the positive control and the control GIC, indicating *S. sanguinis* growth inhibition. The lag phase was observed at the 0−4th h. This phase involved the adaptation of *S. sanguinis* to the new environment. In the log phase, during the 5th to the 9th h, the *S. sanguinis* started to grow and proliferate. The growth curve of the GIC-HCD1 and GIC-HCD2 of F2 and F7 deviated from their respective control groups at this phase, demonstrating the response of HCD to the bacteria. Subsequently, the bacterial growth began to slow until it reached the stationary phase within the 10−11th h. The observations suggested that the HCD is released into the surrounding aqueous environment, reducing the number of dividing bacteria into the cells and thus slowing bacterial growth. After being treated for 11 h, the HCD lessened the number of *S. sanguinis* by 5−11 %, indicating that HCD possesses the potential to inhibit bacterial growth. A remarkable *S. sanguinis* morphological change on GIC-HCD2 F2 was observed (Figure 6(c)), where the bacterial cells appeared shrunken and lost their normal spherical size. The results suggested that the bacterial cell walls were damaged, indicating an optimal antibacterial activity at 2 %.

The potential of HCD in the GICs has been proven in the study. Although only a small amount of HCD was released, the findings clearly showed that HCD was effective in enhancing fluoride release and improving the antibacterial properties of the GICs. The ability to release fluoride ions with additional antibacterial agents is beneficial, as this combination could reduce the severity and frequency of secondary caries.[41] The dual functionality of GIC-HCD presents a significant advantage over other antibacterial agents such as chlorhexidine gluconate,[41] copper nanoparticles,[6] and graphene-silver nanoparticles,[8] which primarily enhance the antibacterial properties but lack documented effects on fluoride release. Furthermore, these antibacterial agents have been explored exclusively with conventional GIC, limiting their scope of application. In contrast, HCD has been successfully investigated in both conventional and resin-modified GICs. This broader versatility, combined with its ability to enhance the antibacterial activity and fluoride release, positions HCD as a more robust and effective antibacterial additive compared to other agents.

The enhanced fluoride release and antibacterial properties observed with HCD-incorporated GICs suggest their

potential for improving patient outcomes, particularly in high-risk caries populations, such as pediatric and geriatric patients, where reducing bacterial load and preventing secondary caries is crucial during the disease control phase of treatment. Additionally, GIC-HCD could be advantageous in temporary restorations, cavity lining and as a base material for deep lesions, further supporting their clinical applications. However, despite these promising results, clinical translation poses challenges, including the need for consistent HCD release over time and the prevention of premature material degradation in the oral environment.

While the incorporation of HCD has successfully enhanced fluoride release and antibacterial properties, which is considered the greatest strength of this study, the mechanical properties of GIC-HCD also warrant further investigation. However, several limitations remain, as the study may not account for the long-term effects of HCD incorporation, such as sustained release of fluoride and prolonged antibacterial activity. Additionally, given the complexity of the oral environment, further testing against a broader range of oral bacteria is essential to gain a more comprehensive understanding of the efficacy of HCD in GICs. Thus, further investigations are necessary to ensure its performance meets standard requirements and provides long-term benefits.

Conclusion

The present study successfully incorporated HCD into the F2 RMGIC and F7 cGIC at weight percentages of 1 % and 2 % (w/w), with a more pronounced effect observed in RMGIC (GIC-HCD F2). This incorporation of HCD in both RMGIC and cGIC demonstrated superior release of HCD and fluoride, as well as improved antibacterial properties at a higher HCD percentage, demonstrating the potential of reducing the severity of secondary caries.

Source of funding

This work was supported by the Universiti Sains Malaysia Grant Scheme RUI 1001/PPSG/813076. The first author received support from the Graduate Fellowship USM Scheme.

Conflict of interest

The authors have no conflict of interest to declare.

Ethical approval

No ethical approval was required for this study.

Authors contributions

All authors contributed equally to this manuscript. NAFA conducted the investigation and wrote the manuscript. FSAR validated the experimental design. ZM and DM provided supervision, reviewed and edited the manuscript. YJ and OBA reviewed the manuscript. All authors have critically reviewed and approved the final draft, and are responsible for the content and similarity index of the manuscript.

Acknowledgment

The authors would like to acknowledge the facilities provided by the Craniofacial Science Laboratory and Biomaterials Science Laboratory of the School of Dental Sciences and Institute for Research in Molecular Medicine (INFORMM), Universiti Sains Malaysia Health Campus.

References

1. Tam L, Chan G, Yim D. In Vitro caries inhibition effects by conventional and resin-modified glass-ionomer restorations. **Operat Dent 1997**; 22: 4–14.
2. Mazzaoui SA, Burrow MF, Tyas MJ. Fluoride release from glass ionomer cements and resin composites coated with a dentin adhesive. **Dent Mater 2000**; 16: 166–171.
3. Ge KX, Quock R, Chu CH, et al. The preventive effect of glass ionomer restorations on new caries formation: a systematic review and meta-analysis. **J Dent 2022**; 125: 104272.
4. Lohbauer U. Dental glass ionomer cements as permanent filling materials? -Properties, limitations and future trends. **Materials 2010**; 3: 76–96.
5. Wiegand A, Buchalla W, Attin T. Review on fluoride-releasing restorative materials-Fluoride release and uptake characteristics, antibacterial activity and influence on caries formation. **Dent Mater 2007**; 23: 343–362.
6. Aguilar-Perez D, Vargas-Coronado R, Cervantes-Uc JM, et al. Antibacterial activity of a glass ionomer cement doped with copper nanoparticles. **Dent Mater J 2020**; 39: 389–396.
7. Alatawi RAS, Elsayed NH, Mohamed WS. Influence of hydroxyapatite nanoparticles on the properties of glass ionomer cement. **J Mater Res Technol 2019**; 8: 344–349.
8. Chen J, Zhao Q, Peng J, et al. Antibacterial and mechanical properties of reduced graphene-silver nanoparticle nanocomposite modified glass ionomer cements. **J Dent 2020**; 96:103332.
9. Kurt A, Tüzüner T. Baygın. Antibacterial characteristics of glass ionomer cements containing antibacterial agents: an in vitro study. **Eur Arch Paediatr Dent 2021**; 22: 49–56.
10. Tüzüner T, Dimkov A, Nicholson JW. The effect of antimicrobial additives on the properties of dental glass-ionomer cements: a review. **Acta Biomater Odontol Scand 2019**; 5: 9–21.
11. Qiu W, Zhou Y, Li Z, et al. Application of antibiotics/antimicrobial agents on dental caries. **BioMed Res Int 2020**: 1–11.
12. ten Cate JMB. The need for antibacterial approaches to improve caries control. **Adv Dent Res 2009**; 21: 8–12.
13. Flores-Morales V, Villasana-Ruiz AP, Garza-Veloz I, et al. Therapeutic effects of coumarins with different substitution patterns. **Molecules 2023**; 28: 1–31.
14. Peng X-M, Damu GL, Zhou C-H. Current developments of coumarin compounds in medicinal chemistry. **Curr Pharmaceut Des 2013**; 19: 3884–3930.
15. Sahoo CR, Sahoo J, Mahapatra M, et al. Coumarin derivatives as promising antibacterial agent(s). **Arab J Chem 2021**; 14: 1–58.
16. Martin ALAR, De Menezes IRA, Sousa AK, et al. In vitro and in silico antibacterial evaluation of coumarin derivatives against MDR strains of Staphylococcus aureus and Escherichia coli. **Microb Pathog 2023**; 177:106058.
17. Kecel-Gunduz S, Budama-Kilinc Y, Bicak B, et al. New coumarin derivative with potential antioxidant activity: synthesis, DNA binding and in silico studies (Docking, MD, ADMET). **Arab J Chem 2023**; 16:104440.

18. Ferreira AR, Alves DN, Castro RD De, et al. Synthesis of coumarin and homoisoflavonoid derivatives and analogs : the search for new antifungal agents. **Pharmaceuticals 2022**; 15: 1−29.
19. Singh A, Diwaker M, Thakur A, et al. Regioselective Pd-catalyzed decarboxylative C-6 acylation of 7-O-carbamate coumarins and their anti-inflammatory evaluation. **Tetrahedron 2023**; 134: 1−9.
20. Rahman FSA, Yusufzai SK, Osman H, et al. Synthesis, characterisation and cytotoxicity activity of thiazole substitution of coumarin derivatives. **J Phys Sci 2016**; 27: 77−87.
21. Aragade P, Maddi V, Khode S, et al. Synthesis and antibacterial activity of a new series of 3-[3-(substituted phenyl)-1-isonicotinoyl-1H-pyrazol-5-yl]-2H-chromen-2-one derivatives. **Arch Pharm Chem Life Sci 2009**; 342: 361−366.
22. Li MK, Li J, Zhou Y, et al. Synthesis, photoluminescent behaviors, and antibacterial activities of 3-acetylcoumarins. **Res Chem Intermed 2015**; 41: 3289−3296.
23. Nasab NH, Azimian F, Kruger HG, et al. Reaction of 3-acetylcoumarin : from methods to mechanism. **Arab J Chem 2023**; 16: 1−72.
24. Klimek MMK, Pitucha M, Woś M, et al. Synthesis, antibacterial and antiproliferative potential of some new 1-pyridinecarbonyl-4-substituted thiosemicarbazide derivatives. **Med Chem Res 2016**; 25: 1666−1677.
25. Fareed MA, Stamboulis A. Nanoclay addition to a conventional glass ionomer cements: influence on physical properties. **Eur J Dermatol 2014**; 8: 456−463.
26. Palmer G, Jones FH, Billington RW, et al. Chlorhexidine release from an experimental glass ionomer cement. **Biomaterials 2004**; 25: 5423−5431.
27. Crisp S, Wilson AD. Reactions in glass ionomer cements: I. Decomposition of the powder. **J Dent Res 1974**; 53: 1408−1413.
28. Meryon SD, Smith AJ. A comparison of fluoride release from three glass ionomer cements and a polycarboxylate cement. **Int Endod J 1984**; 17: 16−24.
29. Paschoal MAB, Gurgel CV, Rios D, et al. Fluoride release profile of a nanofilled resin-modified glass ionomer cement. **Braz Dent J 2011**; 22: 275−279.
30. Sajjad A, Zaripah W, Bakar W, et al. Characterization and efficacy of fluoride elusion of a novel glass ionomer nano zirconia silica hydroxyapatite hybrid material. **Fluoride 2019**: 1−10.
31. Garcez RMVDB, Buzalaf MAR, De Araújo PA. Fluoride release of six restorative materials in water and pH-cycling solutions. **J Appl Oral Sci 2007**; 15: 406−411.
32. Verbeeck RMH, De Maeyer EAP, Marks LAM, et al. Fluoride release process of (resin-modified) glass-ionomer cements versus (polyacid-modified) composite resins. **Biomaterials 1998**; 19: 509−519.
33. Forsten L. Fluoride release and uptake by glass-ionomers and related materials and its clinical effect. **Biomaterials 1998**; 19: 503−508.
34. Kuhn AT, Wilson AD. The dissolution mechanisms of silicate and glass-ionomer dental cements. **Biomaterials 1985**; 6: 378−382.
35. Pitts NB, Zero DT, Marsh PD, et al. Dental caries primer. **Nat Rev Dis Prim 2017**; 3: 1−16.
36. Hengtrakool C, Pearson GJ, Wilson M. Interaction between GIC and S. sanguis biofilms: antibacterial properties and changes of surface hardness. **J Dent 2006**; 34: 588−597.
37. Zhou X, Li Y. *Atlas of oral microbiology from healthy microflora to oral disease*. Zhiejang University Press; 2015.
38. Hafshejani TM, Zamanian A, Venugopal JR, et al. Antibacterial glass-ionomer cement restorative materials: a critical review on the current status of extended release formulations. **J Contr Release 2017**; 262: 317−328.
39. Valadbeigi E, Ghodsi S. Synthesis and characterization of some new thiazolidinedione derivatives containing a coumarin moiety for their antibacterial and antifungal activities. **Med Chem 2017**; 7: 178−185.
40. Boeckh C, Schumacher E, Podbielski A, et al. Antibacterial activity of restorative dental biomaterials in vitro. **Caries Res 2002**; 36: 101−107.
41. Marti LM, Azevedo ER, Da Mata M, et al. Effect of chlorhexidine gluconate on porosity and compressive strength of a glass ionomer cement. **Rev Odontol UNESP 2014**; 43: 236−240.

How to cite this article: Azlisham NAF, Rahman FSA, Mahmood Z, Mohamad D, Johari Y, Al-Batayneh OB. Comparative analysis of hydrazinyl coumarin derivative incorporation in resin-modified and conventional glass ionomer cement. J Taibah Univ Med Sc 2024;19(6):1119−1129.